frontiers | Frontiers in Energy Research

TYPE Original Research
PUBLISHED 14 September 2023
DOI 10.3389/fenrg.2023.1271377

OPEN ACCESS

EDITED BY
Peng Tan,
CNPC Engineering Technology R&D Company Limited, China

REVIEWED BY
Jingshou Liu,
China University of Geosciences Wuhan, China
Shuai Yin,
Xi'an Shiyou University, China

*CORRESPONDENCE
Wei Ju,
wju@cumt.edu.cn

RECEIVED 02 August 2023
ACCEPTED 04 September 2023
PUBLISHED 14 September 2023

CITATION
Yin G, Wu K, Ju W, Qin Y, Qian Z, Xu K, Lu Z, Wang P, Liang X and Liang Y (2023), *In-situ* stress prediction in ultra-deep carbonate reservoirs of Fuman Oilfield, Tarim Basin of China.
Front. Energy Res. 11:1271377.
doi: 10.3389/fenrg.2023.1271377

In-situ stress prediction in ultra-deep carbonate reservoirs of Fuman Oilfield, Tarim Basin of China

Guoqing Yin[1,2], Kongyou Wu[1], Wei Ju[3]*, Yun Qin[2], Ziwei Qian[2], Ke Xu[2], Zhongyuan Lu[2], Peng Wang[2], Xiaobai Liang[3] and Yan Liang[3]

[1]School of Geosciences, China University of Petroleum, Qingdao, Shandong, China, [2]Tarim Oilfield Company, PetroChina, Korla, Xinjiang, China, [3]School of Resources and Geosciences, China University of Mining and Technology, Xuzhou, Jiangsu, China

The Fuman Oilfield in Tarim Basin has great potential for ultra-deep carbonate oil and gas resources, and is an important area for future storage and production increase. The present-day *in-situ* stress field is critical during the exploration and development. However, no systemic investigations have been carried out in this oilfield. Therefore, in this study, the present-day *in-situ* stress field in the Ordovician carbonate reservoir is predicted and analyzed based on well log calculation and geomechanical numerical modeling. The results indicate that, 1) NE-SW-trending is the dominant horizontal maximum principal stress (S_{Hmax}) orientation. The vertical principal stress is the maximum principal stress, showing the Ordovician reservoir is under a normal faulting stress regime. 2) The distribution of *in-situ* stresses in the Ordovician carbonate reservoir is heterogeneous, which is mainly controlled burial depth and fault/fracture development. High stress magnitudes in the Yingshan Formation are mainly in the southeastern part of Fudong area, Fuman Oilfield. The present-day horizontal differential stress mainly ranges from 27 MPa to 30 MPa in the Yingshan carbonate reservoir. iii) Natural fractures are generally stale under the present-day *in-situ* stress state. Fractures that parallel to the S_{Hmax} orientation with high fracture dip angle are easier to be reactivated. The results are expected to provide geomechanical references for further oil and gas development in the Fuman Oilfield of Tarim Basin.

KEYWORDS

geomechanical modeling, Fudong area, *in-situ* stress, Fuman Oilfield, mechanical earth model

1 Introduction

Carbonate formations are the most important type of hydrocarbon reservoirs (Kargarpour, 2020). Aljuboori et al. (2019) reported that 70% of conventional oil reserves in the Middle East lies in carbonate reservoirs. Commonly, in many cases, carbonate reservoirs are tight, hence, it is highly recommended to apply an efficient well stimulation, e.g., acid or hydraulic fracturing. The outcome of hydraulic fracturing largely depends on rock mechanical property, the presence of natural fractures, and most importantly, variations of present-day *in-situ* stresses. The orientation of horizontal maximum principal stress (S_{Hmax}) affects the propagation direction of hydraulic fractures, controls the aperture and permeability of natural fractures within reservoirs (Finkbeiner et al., 1997; Ju et al., 2020a). Besides, due to

the heterogeneity of stress field, wells may not be stimulated equally. As a result, many fields including unconventional oil and gas exploration and development, drilling and completion engineering, borehole stability assessment, optimal well trajectory determination, hydraulic fracturing stimulation plan, etc., benefit from a better understanding of the present-day *in-situ* stress state (Reynolds et al., 2003; Zoback, 2007; Pitcher and Davis, 2016; Rajabi et al., 2016; Ju et al., 2017; Ju et al., 2018; Ju et al., 2020b; Liu et al., 2017;

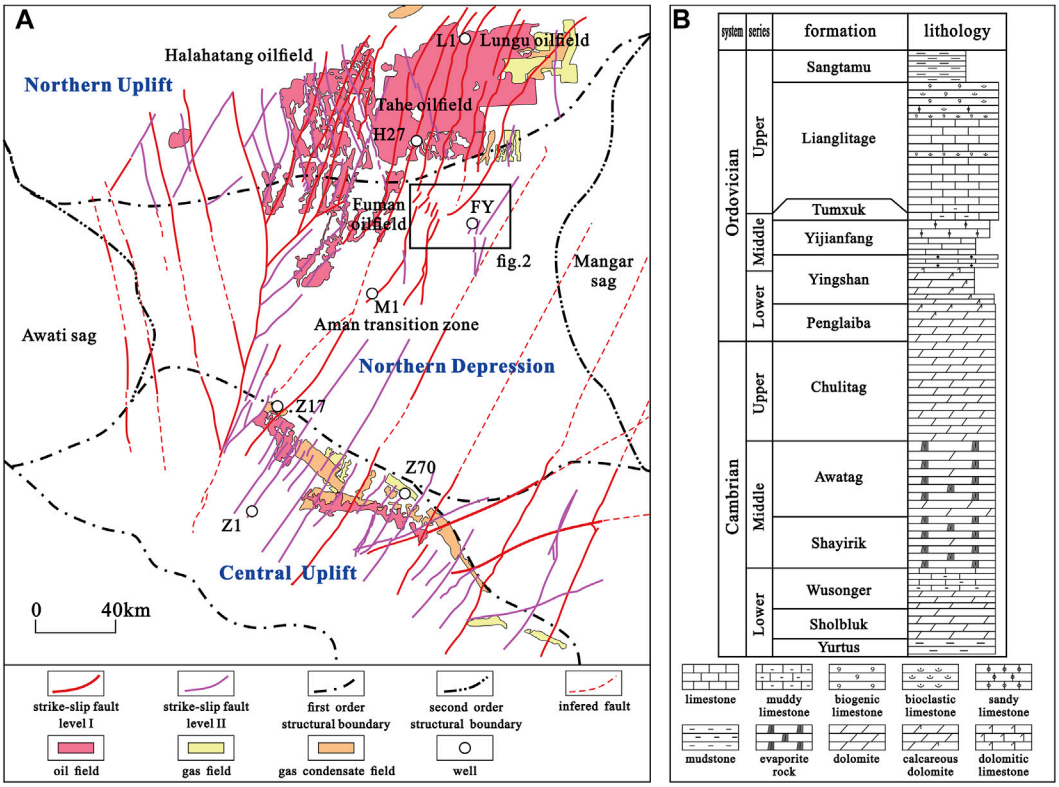

FIGURE 1
(A) The strike-slip fault system in the Ordovician carbonates of Tarim Basin; **(B)** the Cambrian-Ordovician stratigraphic column in the Tarim Basin (after Zhu et al., 2022).

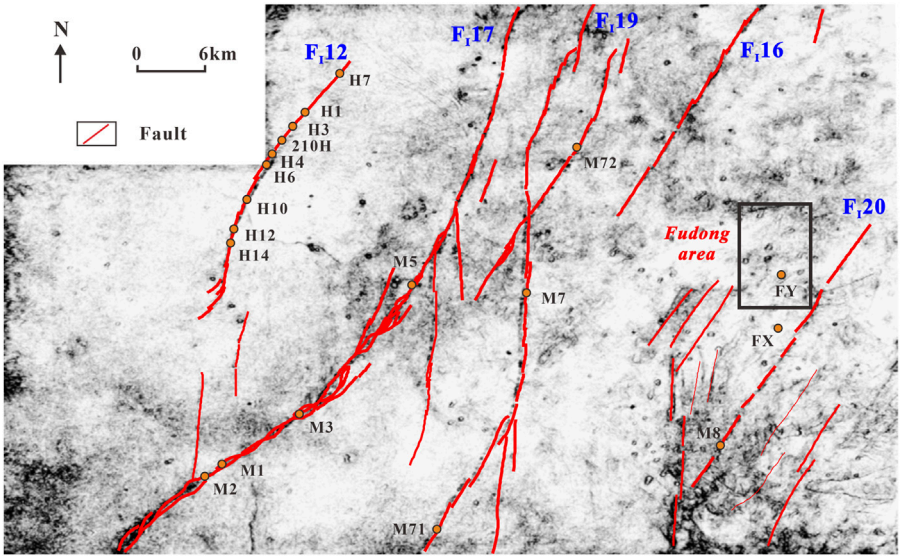

FIGURE 2
The coherent attribute and fault distribution in the Yingshan Formation third member of Fuman Oilfield.

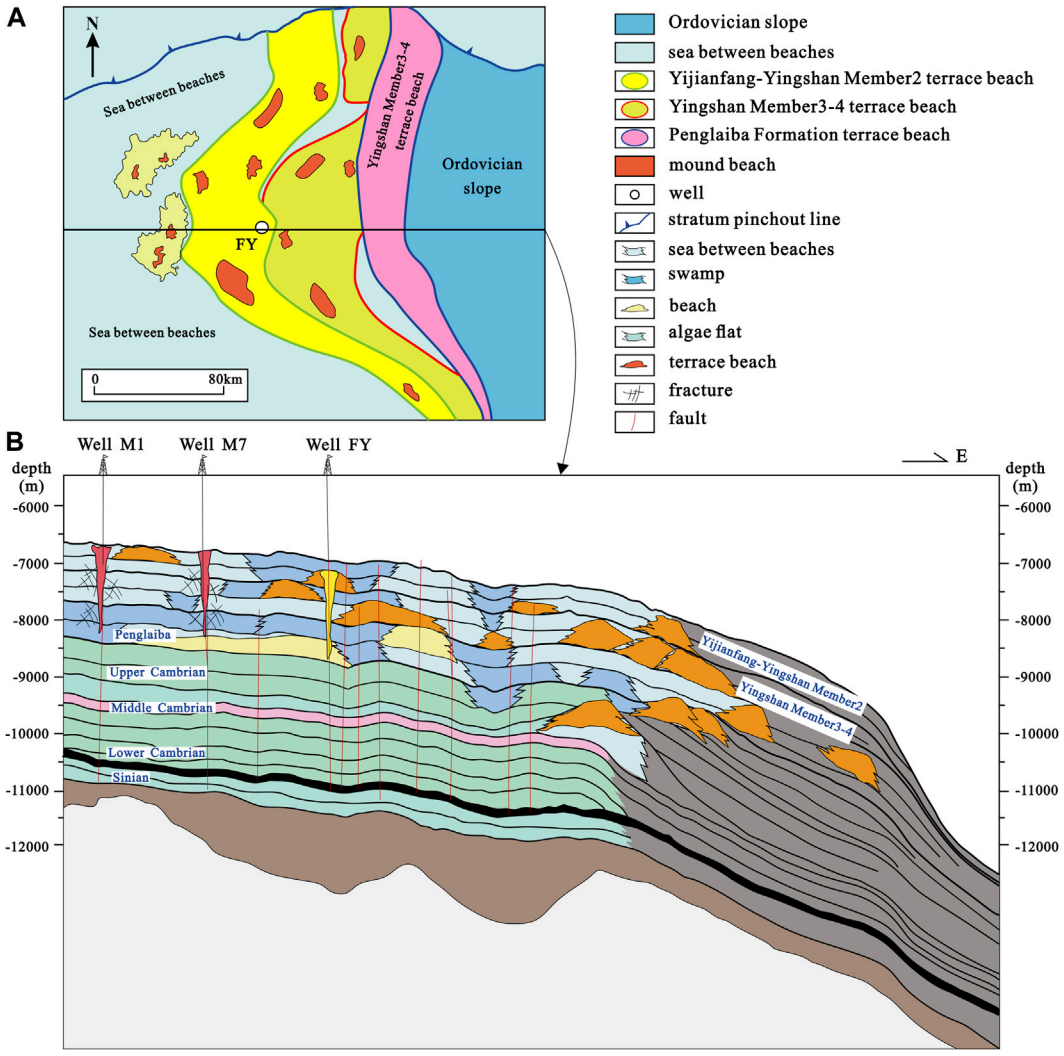

FIGURE 3
Superposition of high-energy platform marginal beach **(A)** and sedimentary microfacies map **(B)** in the Fudong area of Tarim Basin (after Wang et al., 2023).

Yin et al., 2019; Tan et al., 2021; Dontsov, 2022; Yong et al., 2022; Huang et al., 2023).

In-situ stress contains gravitational and tectonic stress. Commonly, in many sedimentary basins, *in-situ* stress can be expressed as three principal stresses, namely, the S_{Hmax}, vertical principal stress (S_v), and the horizontal minimum principal stress (S_{hmin}). Furthermore, based on the relative magnitude of S_{Hmax}, S_v and S_{hmin}, three types of stress regime can be divided (Anderson, 1951):

i, normal faulting stress regime, $S_v > S_{Hmax} > S_{hmin}$;
ii, strike-slip faulting stress regime, $S_{Hmax} > S_v > S_{hmin}$;
iii, reverse faulting stress regime, $S_{Hmax} > S_{hmin} > S_v$.

The deep Cambrian-Ordovician carbonate rocks in the Tarim Basin are enriched with hydrocarbon resources, which serves as a critical field for increasing oil and gas reserves and production (Yang et al., 2020; Ma et al., 2022). In the Tarim Basin, oil and gas resources in these carbonate reservoirs are estimated to be 70×10^8 tons, and are mainly controlled by strike-slip faults (Li et al., 2020; Jia et al., 2022). However, carbonate rocks in the Tarim Basin are deep and ultra-deep buried, generally form a tight reservoir, and hydrocarbon distributions are complicated, which limits the economic development (Zhu et al., 2022). With the improvement of technology and theory, since the year 2020, many large oil and gas discoveries have been successively made in carbonate reservoirs of Tarim Basin. Well M 1 is a discovery well of fault-controlled reservoir with high single well production. In the Ordovician Yijianfang Formation with a burial depth of over 7,535 m, the tested oil and gas production reach approximately 624 m^3/d and 37.13×10^4 m^3/d, respectively (Yang et al., 2020). Further, the exploration direction of ultra-deep carbonate oil and gas resources in the platform area turns to fracture-controlled and reef-beach type reservoirs, which have become a major drilling target. Recently, Well Fudong 1 was successfully drilled in the Fuman Oilfield, which confirms that the high-energy platform marginal shoal with secondary network faults has the capacities of reservoir development and hydrocarbon accumulation. This finding breaks through the exploration forbidden zone in ultra-deep high-energy shoal carbonate rocks with the burial depth of greater than 8,000 m, and

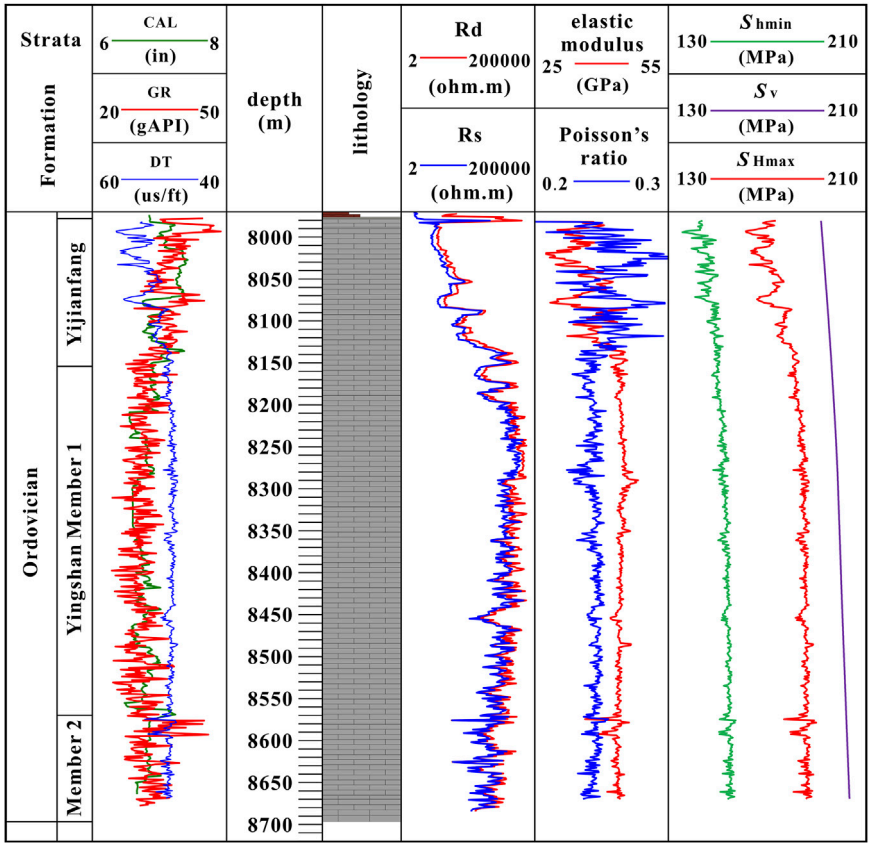

FIGURE 4
The 1D MEM in the Ordovician reservoir of Well FX.

expands the understanding on hydrocarbon accumulation pattern in carbonate reservoirs (Wang et al., 2023).

In the Tarim Basin, the carbonate reservoirs commonly show strong heterogeneity due to the development of strike-slip faults, fault-related natural fractures, caves and vugs. As a result, the development of this type of reservoir faces problems of large variation in single-well production capacity. Besides, complex present-day *in-situ* stress system and reservoir pressure cause difficult drilling operation and frequent incidents, and it is difficult to optimize effective measures for well completion (Yang et al., 2018). Understanding well of the *in-situ* stress field can help better deal with and solve the above problems (Zhao et al., 2020).

Prior to this analysis, distribution of present-day *in-situ* stress in ultradeep carbonate reservoirs of Fuman Oilfield, especially the Fudong area, has not been the subject of any systematical investigations, which limits the further development. Therefore, to improve the development efficiency, the present-day *in-situ* stress section was built, spatial distributions were predicted based on geomechanical models in this study. The results are expected to provide *in-situ* stress references for high-efficient development.

2 Geological setting

The Fuman Oilfield is located in the Northern Depression of Tarim Basin, between the Northern Uplift and Central Uplift (Figure 1A), which is the largest ultra-deep-sea facies fractured cave-type carbonate reservoir discovered in China. The petroleum geological reserves exceed 1×10^9 tons, and the annual oil production has more than 2×10^6 tons (Wang et al., 2021). The carbonate reservoirs in Fuman Oilfield are generally at ultra-depth of 7,500 m–10,000 m, and the main oil producing layer is the Ordovician Yijianfang Formation to Yingshan Formation (Figure 1B). The reservoir has huge exploration potential and development benefits. The largest thickness of the reservoir is 550 m, and the highest oil production is more than 1,600 m^3/d. Overall, it has the features of ultra-deep, ultra-high temperature, and ultra-high pressure that are rare in the world (Zhu et al., 2022; Wang et al., 2023). For the Fuman Oilfield, traditional oil and gas geology theories are basically "not applicable", conventional drilling techniques are basically "unsuccessful", and the exploration and development are extremely difficult.

The distributions of carbonate reservoirs in Fuman Oilfield are controlled by large strike-slip faults. During multiple tectonic movements, these faults have evolved into the current structure pattern through regeneration, inheritance, superposition, and transformation, showing the features of longitudinal stratification, planar zoning, and segmentation along the strike (Tian et al., 2021; Jia et al., 2022; Zhu et al., 2022; Figure 2).

The formation and internal configuration of strike-slip faults are affected by regional tectonic stress. Strike-slip faults in the Fuman Oilfield have experienced at least three stages, namely, the Middle Caledonian stage, the Late Caledonian stage, and the Middle-Late

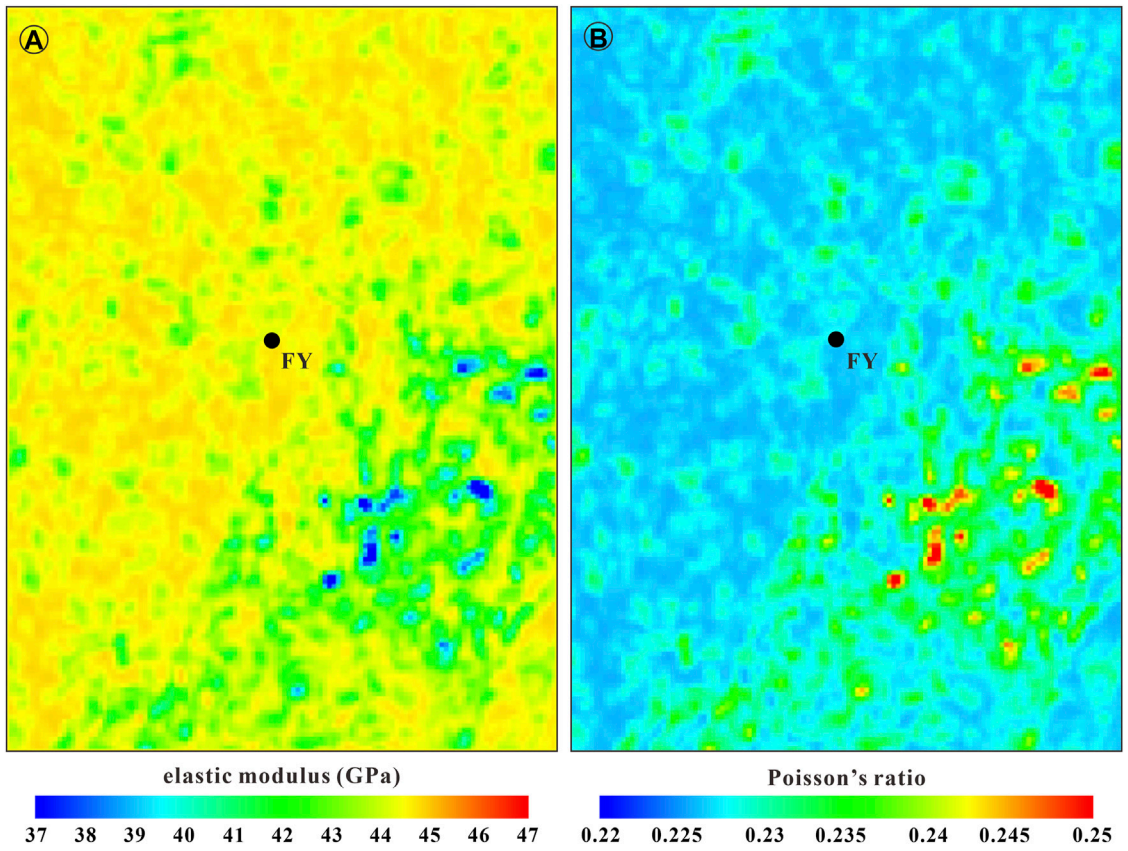

FIGURE 5
Mechanical properties used in the FE numerical model of Fudong area, Fuman Oilfield **(A)** elastic modulus; **(B)** Poisson's ratio.

Hercynian stage. Different fracture assemblages were formed due to the differences in the kinetic mechanisms underlying each active phase, which in turn controlled the differential oil and gas accumulation patterns (Jia et al., 2022; Wang et al., 2022).

In the Fuman Oilfield, the Fudong area is located within a platform margin high energy beach body (Figure 3). Structural paleo-geographical environment is also favorable for the development of platform margin high-energy shoals. Besides, the development of secondary network faults reforms the reservoir and provide favorable transport conditions. Taking Well Fudong 1 as an example, well testing shows that there are totally 13 layers with a thickness of 41.95 m in the Yijianfang Formation-Yingshan Formation. The second member of Yingshan Formation is extremely great. The estimated reservoir pressure is 175.21 MPa, pressure coefficient is approximately 2.1, which indicates an ultra-high pressure condensate gas reservoir.

3 Method and parameters

3.1 One dimensional (1D) mechanical Earth model (MEM)

Generally, the 1D MEM is built to analyze the variations of three principal stress magnitudes (S_v, S_{Hmax} and S_{hmin}) with burial depth. The S_v can be easily calculated and determined based on the integration of rock density from the ground surface to a specific depth (Eq.1; Zoback et al., 2003; Ju et al., 2017).

$$S_v = \int_0^z \rho(z) g \, dz \tag{1}$$

where S_v is the vertical principal stress, g is the gravitational acceleration, z is the burial depth from surface to a specific depth, $\rho(z)$ is the density of overburden as a function of burial depth.

Actually, no density logs and velocity data are obtained from the ground level during well log measurement. Hence, in this study, a S_v gradient of approximately 23,500 Pa/m was used from ground surface to the depth with the first density value.

In this study, magnitudes of S_{Hmax} and S_{hmin} are calculated using poroelastic stress equations (Thiercelin and Plumb, 1994; Eqs. 2, 3):

$$S_{Hmax} = \frac{\mu}{1-\mu}(S_v - \alpha P_o) + \alpha P_o + \frac{E}{(1-\mu)^2}(\varepsilon_{max} + \mu\varepsilon_{min}) \tag{2}$$

$$S_{hmin} = \frac{\mu}{1-\mu}(S_v - \alpha P_o) + \alpha P_o + \frac{E}{(1-\mu)^2}(\varepsilon_{min} + \mu\varepsilon_{max}) \tag{3}$$

where μ is the static Poisson's ratio, E is the static Young's modulus, ε_{max} is the strain in the maximum stress direction, ε_{min} is the strain in the minimum stress direction, P_o is the pore pressure, and α is the Biot's coefficient.

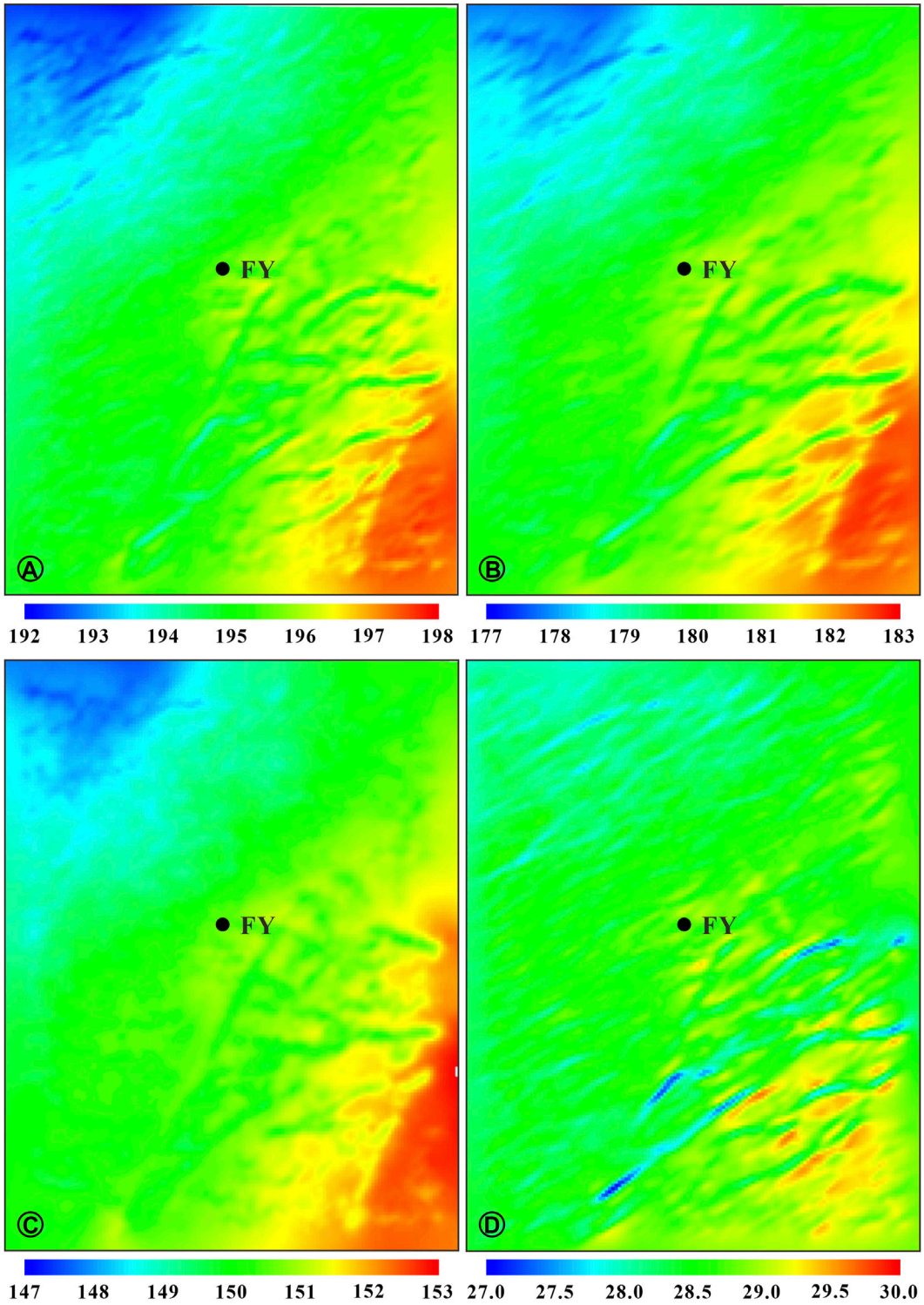

FIGURE 6
Stress spatial distribution in the Ordovician Yingshan Formation reservoir of Fudong area **(A)** S_v; **(B)** S_{Hmax}; **(C)** S_{hmin}; **(D)** horizontal stress difference; unit: MPa.

The α is calculated based on an empirical equation (Eq.4):

$$\alpha = 1 - \exp\left(7.5 \tan \frac{\varphi\pi}{2}\right) \quad (4)$$

where φ is the porosity of the rock, which can be obtained from laboratory experiments or well log calculations.

Commonly, the ε_{max} and ε_{min} are unable to be obtained directly. Parameters of the E, μ, P_o, and α can be measured from experiments or empirical formula. The S_{Hmax} and S_{hmin} magnitudes may be calculated based on hydraulic fracturing. Hence, in this study, parameters of ε_{max} and ε_{min} could be obtained inversely based on Eqs. 2, 3.

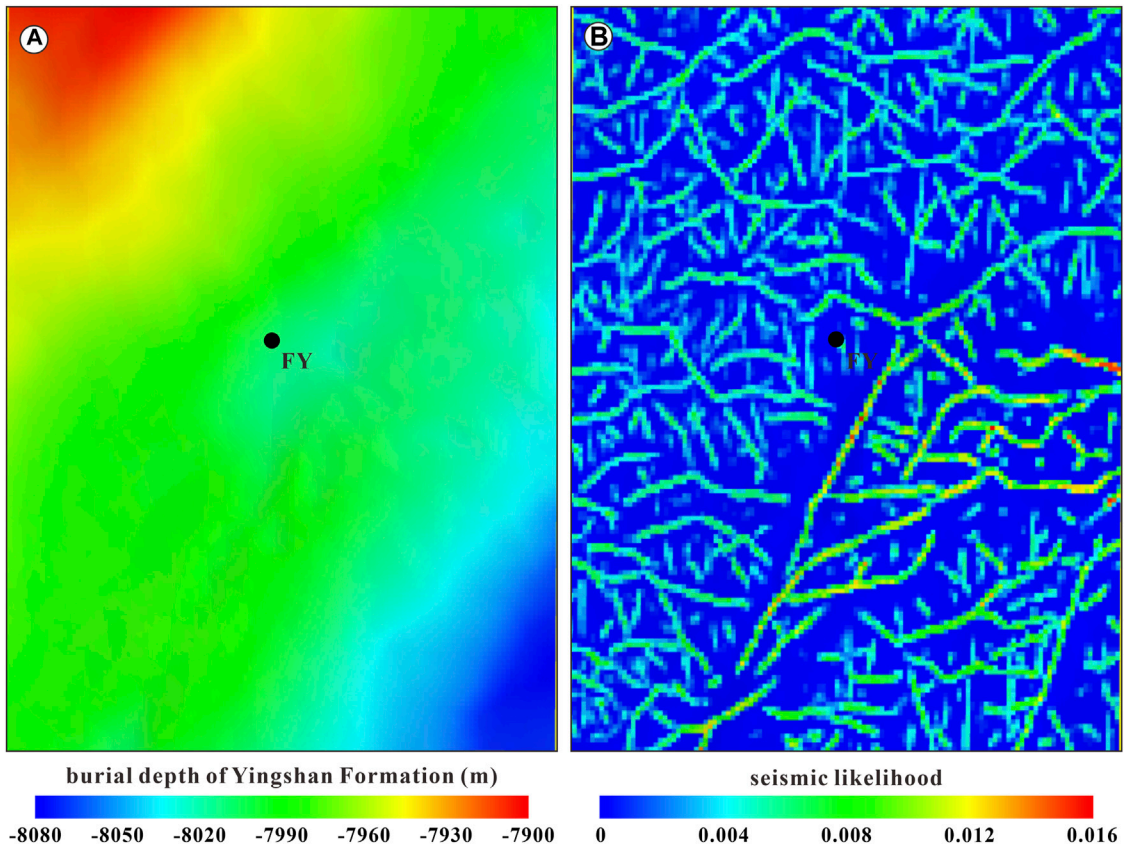

FIGURE 7
Burial depth **(A)** and seismic likelihood **(B)** of Yingshan Formation in the Fudong area of Fuman Oilfield.

3.2 *In-situ* stress finite element (FE) numerical modeling

In the study area, there are only three drilling wells, which limits the further understanding on spatial distribution of present-day *in-situ* stresses. Hence, the FE numerical modeling technique and FracMAN code are utilized to investigate the present-day *in-situ* stress distribution in the carbonate reservoirs of Fudong area.

During the FE numerical modeling, all geological bodies are discretized into finite continuous elements that are connected by nodes in accordance with the fundamental principle of the FE modeling approach. The entire region's field function is converted into a node function including fundamental variations in stress, strain, and displacement resulted from external forces (Ding et al., 2012; Liu et al., 2017).

Theoretically, based on the principle of virtual displacement, the relationship among nodal displacement, integral nodal load and integral stiffness follows Eq. 5.

$$[F] = [K][\delta] \tag{5}$$

where $[F]$ is the integral nodal load matrix, $[\delta]$ is the nodal displacement matrix for the integral structure of the examined elemental array, and $[K]$ is the integral stiffness matrix.

The matrix form can be derived as follows (Eq.6).

$$[\varepsilon] = [B][\delta] \tag{6}$$

where $[\delta]$ is the nodal displacement matrix, $[B]$ is the geometric matrix.

From the physical equation, stress and strain can be expressed as Eq. 7:

$$[\sigma] = [D][\varepsilon] \tag{7}$$

where $[D]$ is the elasticity matrix, σ is the stress, and ε is the strain.

The modeling process involves the following three steps: 1) determining the geometric shapes and characteristics of strata, 2) determining the spatial distributions of mechanical properties, and 3) determining the loading pattern for geological bodies within the model, and the associated boundary conditions.

4 Results

4.1 The 1D MEM in the Fuman Oilfield

Stress variations with burial depth are calculated and plotted in Figure 5. The S_v, S_{Hmax} and S_{hmin} magnitudes vary from 191.90 MPa to 198.98 MPa, 160.33 MPa–190.38 MPa, and 134.35 MPa–157.51 MPa, respectively, in the Yingshan carbonate reservoir. The S_{Hmax} and S_{hmin} magnitudes slightly change with depth, which may be influenced by factors of natural fracture development and bedding. Overall, the S_v and S_{hmin} are the maximum and minimum principal stress (Figure 4), following the relationship of $S_v > S_{Hmax} > S_{hmin}$, indicating a normal

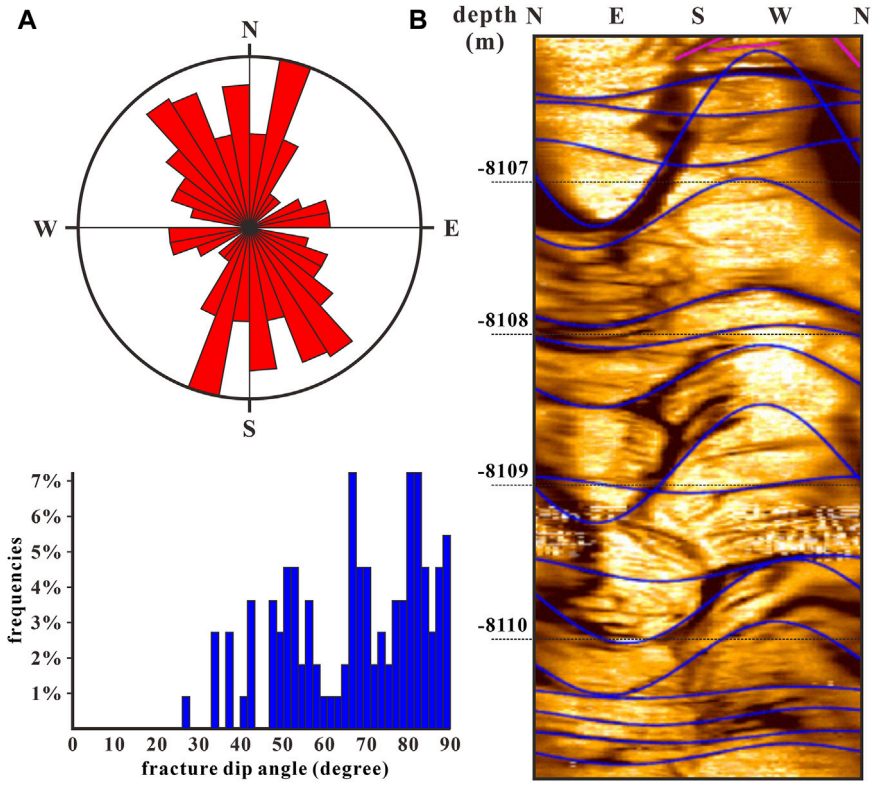

FIGURE 8
Characteristics of natural fractures in the carbonate reservoirs of Well M7 in Fuman Oilfield. **(A)** fracture strike and dip angle; **(B)** imaging log showing natural fractures.

faulting stress regime in the Yingshan carbonate reservoir of Fudong area.

4.2 Spatial distribution of present-day *in-situ* stresses

The initial three dimensional (3D) geometric model was built using the Petrel platform based on geological information obtained from seismic interpretation. The 3D reservoir grid was created using pillar gridding, makeup horizons and layering.

In this study, each element has the proper mechanical properties assigned to it (Figure 5). The elastic modulus in the Yingshan carbonate reservoir mainly ranges from 37 GPa to 47 GPa. The Poisson's ratio varies between 0.22 and 0.25 in the Yingshan Formation of Fudong area.

Generally, many methods can be used to determine the S_{Hmax} orientation, including interpretations from wellbore breakouts (BOs) and drilling-induced fractures (DIFs), focal mechanism analysis, etc. (Zoback et al., 2003; Heidbach et al., 2010; Rajabi et al., 2016; Ju et al., 2020a). In this study, the present-day S_{Hmax} orientation was analyzed from BOs and DIFs, which is approximately NE60° on average in the Yijianfang-Yingshan Formation of Fuman Oilfield. The orientation is consistent with the strike-slip fault direction. The Fuman Oilfield is controlled by the NE–SW horizontal tectonic compressive stress field.

It is unrealistic to place the loading conditions directly into each of the reservoir grid. Generally, there are three types of boundary conditions, namely, gravity, initialization and explicit initialization. In this study, the far field boundary condition was used for FE modeling with initialization method, which calculates the initial stress using the ratio of horizontal stresses and vertical stress. Based on calculated 1D MEM in the Ordovician reservoir of Fuman Oilfield, in the numerical model, the S_v gradient is 0.0235 MPa/m, the S_{Hmax}/S_v ratio is 0.921, and the S_{hmin}/S_v ratio is 0.769. The present-day S_{Hmax} orientation is set NE60°.

The results indicate that the S_v ranges from 192 MPa to 198 MPa, the S_{Hmax} magnitude is between 177 MPa and 183 MPa, the S_{hmin} magnitude varies from 147 MPa to 153 MPa (Figure 6). Their relationship follows $S_v > S_{Hmax} > S_{hmin}$, indicating a normal faulting stress regime. All the three principal stresses show similar distribution pattern, high and low stress magnitudes are mainly in the southeastern and northwestern part of Fudong area, respectively.

The overall distribution pattern is mainly controlled by burial depth. Larger depth produces higher stress magnitude (Figure 7A). Detailed variations of stress distribution commonly result from the development minor faults and natural fractures (Figure 7B).

5 Discussions

5.1 Horizontal stress difference

The commercial production of carbonate reservoir frequently requires hydraulic fracturing. The present-day *in-situ* stress state,

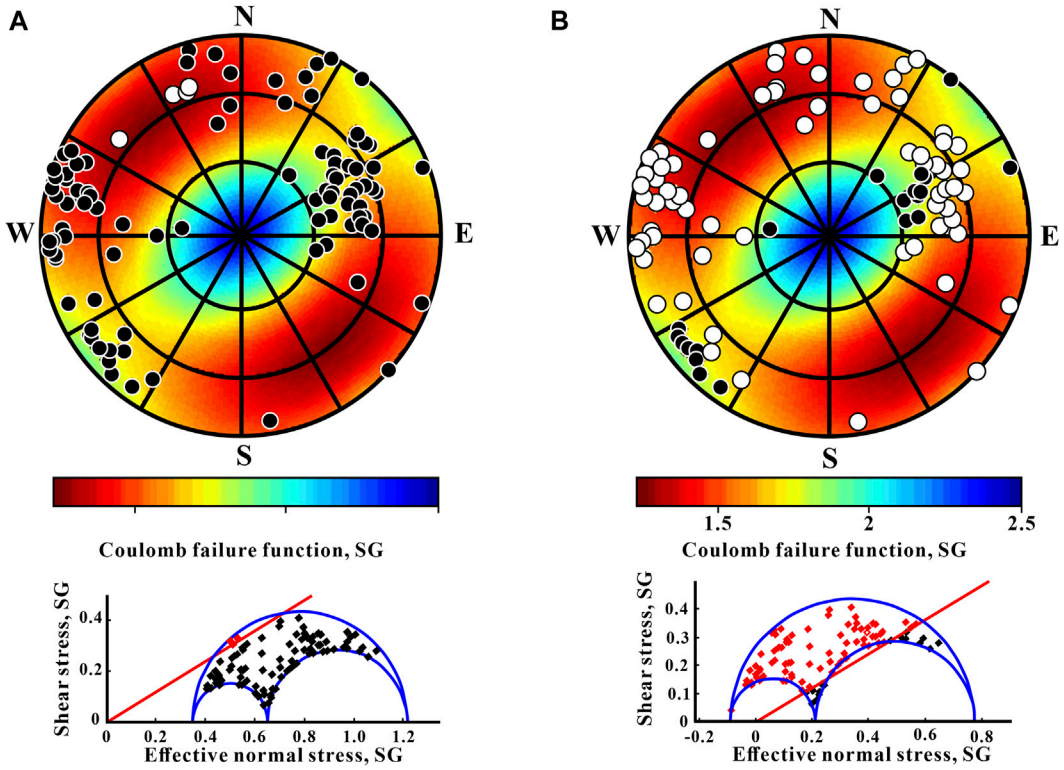

FIGURE 9
Lower hemisphere stereonet plots and three dimensional Mohr circles showing critically stressed natural fractures in the Ordovician carbonate reservoirs of Well M7, Fuman Oilfield **(A)** 1.29 MPa/100 m; **(B)** 1.73 MPa/100 m The fracture orientations are plotted as the pole of planes. The red colors show the high likelihood of fracture reactivation, while the blue colors indicate the low likelihood of reactivation for all possible fractures in the present-day stress state. Black and white dots in the stereonet plots are normal and critically stressed natural fractures, respectively. In the Mohr circles, black and red dots are normal and critically stressed natural fractures. SG is specific gravity.

rock mechanical property and natural fractures may influence the propagation of hydraulic fractures (Zoback, 2007; Ardakani et al., 2017; Ju et al., 2020a). Differential stress is widely used to analyze the propagation pattern of hydraulic fractures, and low stress difference can generate complex hydraulic fracture networks in most cases. Besides, high stress difference may easily cause rock failures, influencing wellbore stability.

Based on the above *in-situ* stress prediction, the present-day horizontal differential stress mainly ranges from 27 MPa to 30 MPa in the Yingshan reservoir. Relatively low values are located in the northwestern part of Fudong area (Figure 6D).

5.2 Coupling effect between *in-situ* stress and natural fracture

In-situ stress state is a significant factor that influences the transmitting ability of natural fractures (Zoback, 2007). When fracture orientations parallel to the present-day S_{Hmax} orientation, fluid flows in natural fractures well be greatly improved. Commonly, hydraulic fracturing process involves increasing the reservoir pressure by injecting high-pressure fluid into the target reservoir, which will cause many geomechanically-induced deformations, including fracture shear slip capacity improvement and natural fracture reactivation (Reynolds et al., 2003). This process plays a positive role in the transportation of oil and gas from the periphery of the well to the wellbore (Xu et al., 2022).

To quantitatively understand and analyze the coupling effect between *in-situ* stress and natural fractures, the "reactivation risk plot" that uses the Mohr's Circle Criterion (Mildren et al., 2002; Rajabi et al., 2016) are introduced to evaluate the risk of natural fracture reactivations in the Ordovician carbonate reservoir of Fuman Oilfield.

In this study, Well M7 is taken as an example, characteristics of natural fractures developed in the Ordovician carbonate rocks of Fuman Oilfield are analyzed based on imaging logs. Fracture strikes mainly range from NW-SE to NNE-SSW (Figure 8A), fracture dip angles are relatively high, the majority of them are higher than 50° (Figure 8B).

Analysis of the coupling effect between *in-situ* stress and natural fractures indicates that natural fractures are generally stable under the present-day *in-situ* stress state. With the injection of fluids into the carbonate rocks, reservoir pressure increases, causing the leftward movement of the Mohr's Circle (Figure 9). Furthermore, those fractures parallel to the S_{Hmax} orientation with high fracture dip angle are easier to be reactivated during the fluid injection process (Figure 9A). When the net bottom reservoir pressure is

1.29 MPa/100 m, four natural fractures are reactivated and become effective with the reactivation rate of 3.63% (Figure 9A). When the net bottom reservoir pressure is 1.73 MPa/100 m, the majority of natural fractures are reactivated, the reactivation rate is approximately 81.82% (Figure 9B).

6 Conclusion

In this study, the present-day *in-situ* stress field in the Ordovician carbonate reservoir of Fuman Oilfield, especially the Fudong area, was analyzed and predicted based on well calculation and geomechanical modeling. The results are expected to provide references in *in-situ* stress for subsequent efficient exploration and development.

The dominant S_{Hmax} orientation is NE-SW-trending (nearly 60°N) in the Yijianfang-Yingshan Formation of Fuman Oilfield. The S_v and S_{hmin} are the maximum and minimum principal stress, respectively, indicating that the Ordovician reservoir is under a normal faulting stress regime.

The present-day *in-situ* stress in the Ordovician reservoir is heterogeneously distributed, mainly controlled by burial depth, fault/natural fracture development and distribution. High stress magnitudes in the Yingshan Formation of Fudong area are mainly in the southeastern part of the study area. The present-day horizontal differential stress mainly ranges from 27 MPa to 30 MPa in the Yingshan carbonate reservoir. Relatively low values are located in the northwestern part of Fudong area.

The strikes of natural fracture in the Ordovician reservoir mainly range from NW-SE to NNE-SSW. Analysis of the coupling effect between *in-situ* stress and natural fractures indicates that natural fractures are generally stable under the present-day *in-situ* stress state. There is a critical value for fractures to be reactivated. Fractures parallel to the S_{Hmax} orientation with high fracture dip angle are easier to be reactivated.

Data availability statement

The raw data supporting the conclusion of this article will be made available by the authors, without undue reservation.

Author contributions

GY: Methodology, Writing–original draft. KW: Supervision, Writing–review and editing. WJ: Conceptualization, Writing–review and editing. YQ: Data curation, Writing–review and editing. ZQ: Data curation, Writing–review and editing. KX: Data curation, Writing–review and editing. ZL: Writing–review and editing, Resources. PW: Writing–review and editing, Resources. XL: Methodology, Writing–review and editing. YL: Methodology, Writing–review and editing.

Funding

The author(s) declare financial support was received for the research, authorship, and/or publication of this article. This study is supported by the Major Scientific and Technological Project of PetroChina Co., Ltd. (2018E-1803). The funder was not involved in the study design, collection, analysis, interpretation of data, the writing of this article, or the decision to submit it for publication.

Acknowledgments

Many thanks to the reviewers for improving this manuscript.

Conflict of interest

Authors GY, YQ, ZQ, KX, ZL, and PW were employed by Tarim Oilfield Company, PetroChina.

The remaining authors declare that the research was conducted in the absence of any commercial or financial relationships that could be construed as a potential conflict of interest.

Publisher's note

References

Aljuboori, F. A., Lee, J. H., Elraies, K. A., and Stephen, K. D. (2019). Gravity drainage mechanism in naturally fractured carbonate reservoirs: review and application. *Energies* 12, 3699. doi:10.3390/en12193699

Anderson, E. M. (1951). *The dynamics of faulting and dyke Formation with applications to britain*. second edition. Edinburgh: Oliver, 206.

Ardakani, E. P., Urbancic, T., Baig, A. M., and Viegas, G. (2017). The influence of bedding-parallel fractures in hydraulic fracture containment. *First Break* 35 (4), 71–76. doi:10.3997/1365-2397.35.4.87844

Ding, W. L., Fan, T. L., Yu, B. S., Huang, X. B., and Liu, C. (2012). Ordovician carbonate reservoir fracture characteristics and fracture distribution forecasting in the Tazhong area of Tarim Basin, Northwest China. *J. Petroleum Sci. Eng.* 86-87, 62–70. doi:10.1016/j.petrol.2012.03.006

Dontsov, E. V. (2022). Analysis of a constant height hydraulic fracture driven by a power-law fluid. *Rock Mech. Bull.* 1 (1), 100003. doi:10.1016/j.rockmb.2022.100003

Finkbeiner, T., Barton, C. A., and Zoback, M. D. (1997). Relationships among *in-situ* stress, fractures and faults, and fluid flow: monterey formation, santa maria basin, California. *AAPG Bull.* 81, 1975–1999.

Heidbach, O., Tingay, M., Barth, A., Reinecker, J., Kurfeß, D., and Muller, B. (2010). Global crustal stress pattern based on the World Stress Map database release 2008. *Tectonophysics* 482, 3–15. doi:10.1016/j.tecto.2009.07.023

Huang, L. K., He, R., Yang, Z. Z., Tan, P., Chen, W. H., Li, X. G., et al. (2023). Exploring hydraulic fracture behavior in glutenite formation with strong heterogeneity and variable lithology based on DEM simulation. *Eng. Fract. Mech.* 278, 109020. doi:10.1016/j.engfracmech.2022.109020

Jia, C. Z., Ma, D. B., Yuan, J. Y., Wei, G. Q., Yang, M., Yan, L., et al. (2022). Structural characteristics, formation & evolution and genetic mechanisms of strizke–slip faults in the Tarim Basin. *Nat. Gas. Ind. B* 9 (1), 51–62. doi:10.1016/j.ngib.2021.08.017

Ju, W., Jiang, B., Miao, Q., Wang, J. L., Qu, Z. H., and Li, M. (2018). Variation of *in situ* stress regime in coal reservoirs, eastern yunnan region, south China: implications for coalbed methane production. *AAPG Bull.* 102 (11), 2283–2303. doi:10.1306/04241817376

Ju, W., Niu, X. B., Feng, S. B., You, Y., Xu, K., Wang, G., et al. (2020b). Predicting the present-day *in situ* stress distribution within the Yanchang Formation Chang 7 shale oil reservoir of Ordos Basin, central China. *Petroleum Sci.* 17, 912–924. doi:10.1007/s12182-020-00448-8

Ju, W., Niu, X. B., Feng, S. B., You, Y., Xu, K., Wang, G., et al. (2020a). Present-day *in-situ* stress field within the Yanchang Formation tight oil reservoir of Ordos Basin, central China. *J. Petroleum Sci. Eng.* 187, 106809. doi:10.1016/j.petrol.2019.106809

Ju, W., Shen, J., Qin, Y., Meng, S. Z., Wu, C. F., Shen, Y. L., et al. (2017). *In-situ* stress state in the linxing region, eastern ordos basin, China: implications for unconventional gas exploration and production. *Mar. Petroleum Geol.* 86, 66–78. doi:10.1016/j.marpetgeo.2017.05.026

Kargarpour, M. A. (2020). Carbonate reservoir characterization: an integrated approach. *J. Petroleum Explor. Prod. Technol.* 10, 2655–2667. doi:10.1007/s13202-020-00946-w

Li, H. Y., Liu, J., Gong, W., Huang, C., and Ren, L. D. (2020). Identification and characterization of strike-slip faults and traps of fault-karst reservoir in the Shunbei area, Tarim Basin. *China Pet. Explor.* 25 (3), 107–120. doi:10.3969/j.issn.1672-7703.2020.03.010 (in Chinese with English abstract)

Liu, J. S., Ding, W. L., Yang, H. M., Wang, R. Y., Yin, S., Li, A., et al. (2017). 3D geomechanical modeling and numerical simulation of *in-situ* stress fields in shale reservoirs: A case study of the lower cambrian niutitang Formation in the cen'gong block, south China. *Tectonophysics* 712-713, 663–683. doi:10.1016/j.tecto.2017.06.030

Ma, Y. S., Cai, X. Y., Yun, L., Li, Z. J., Li, H. L., Deng, S., et al. (2022). Practice and theoretical and technical progress in exploration and development of Shunbei ultra-deep carbonate oil and gas field, Tarim Basin, NW China. *Petroleum Explor. Dev.* 49 (1), 1–20. doi:10.1016/s1876-3804(22)60001-6

Mildren, S. D., Hillis, R. R., and Kaldi, J. (2002). Calibrating predictions of fault seal reactivation in the Timor Sea. *APPEA J.* 42, 187–202. doi:10.1071/aj01011

Pitcher, T., and Davis, T. L. (2016). Geomechanical analysis of *in-situ* stress and its influence on hydraulic fracturing at the Wattenberg field, Colorado. *First Break* 34 (3), 45–50. doi:10.3997/1365-2397.34.3.83974

Rajabi, M., Tingay, M., and Heidbach, O. (2016). The present-day state of tectonic stress in the darling basin, Australia: implications for exploration and production. *Mar. Petroleum Geol.* 77, 776–790. doi:10.1016/j.marpetgeo.2016.07.021

Reynolds, S., Hillis, R., and Paraschivoiu, E. (2003). *In situ* stress field, fault reactivation and seal integrity in the Bight Basin, South Australia. *Explor. Geophys.* 34, 174–181. doi:10.1071/eg03174

Tan, P., Jin, Y., and Pang, H. W. (2021). Hydraulic fracture vertical propagation behavior in transversely isotropic layered shale formation with transition zone using XFEM-based CZM method. *Eng. Fract. Mech.* 248, 107707. doi:10.1016/j.engfracmech.2021.107707

Thiercelin, M. J., and Plumb, R. A. (1994). Core-based prediction of lithologic stress contrasts in east Texas formations. *Soc. Petroleum Eng. Form. Eval.* 9 (4), 251–258. doi:10.2118/21847-pa

Tian, J., Yang, H. J., Zhu, Y. F., Deng, X. L., Xie, Z., Zhang, Y. T., et al. (2021). Geological conditions for hydrocarbon accumulation and key technologies for exploration and development in Fuman Oilfield, Tarim Basin. *Acta Pet. Sin.* 42 (8), 971–985. doi:10.7623/syxb202108001 (in Chinese with English abstract)

Wang, Q. H., Yang, H. J., Wang, R. J., Li, S. Y., and Deng, X. L. (2021). Discovery and exploration technology of fault-controlled large oil and gas fields of ultra-deep formation in strike-slip fault zone in Tarim Basin. *China Pet. Explor.* 26, 58–71. doi:10.3969/j.issn.1672-7703.2021.04.005 (in Chinese with English abstract)

Wang, Q. H., Yang, H. J., Zhang, Y. T., Li, Y., Yang, X. Z., Zhu, Y. F., et al. (2023). Great discovery and its significance in the ordovician in well Fudong 1 in fuman oilfield, Tarim Basin. *China Pet. Explor.* 28 (1), 47–58. doi:10.3969/j.issn.1672-7703.2023.01.005 (in Chinese with English abstract)

Wang, X. T., Wang, J., Cao, Y. C., Han, J., Wu, K. Y., Liu, Y., et al. (2022). Characteristics, formation mechanism and evolution model of Ordovician carbonate fault-controlled reservoirs in the Shunnan area of the Shuntuogole lower uplift, Tarim Basin, China. *Mar. Petroleum Geol.* 145, 105878. doi:10.1016/j.marpetgeo.2022.105878

Xu, K., Yang, H. J., Zhang, H., Ju, W., Li, C., Fang, L., et al. (2022). Fracture effectiveness evaluation in ultra-deep reservoirs based on geomechanical method, Kuqa Depression, Tarim Basin, NW China. *J. Petroleum Sci. Eng.* 215, 110604. doi:10.1016/j.petrol.2022.110604

Yang, H. J., Deng, X. L., Zhang, Y. T., Xie, Z., Li, Y., Li, S. Y., et al. (2020). Great discovery and its significance of exploration for Ordovician ultra-deep fault-controlled carbonate reservoirs of Well Manshen 1 in Tarim Basin. *China Pet. Explor.* 25 (3), 13–23. doi:10.3969/j.issn.1672-7703.2020.03.002 (in Chinese with English abstract)

Yang, H. J., Zhang, H., Yin, G. Q., and Han, X. J. (2018). Geomechanics-based geology-engineering integration boosting high-efficiency exploration of fractured-vuggy carbonate reservoirs: A case study on west yueman block, northern Tarim Basin. *China Pet. Explor.* 23 (2), 27–36. doi:10.3969/j.issn.1672-7703.2018.02.004 (in Chinese with English abstract)

Yin, S., Xie, R. C., Wu, Z. H., Liu, J. S., and Ding, W. L. (2019). *In situ* stress heterogeneity in a highly developed strike-slip fault zone and its effect on the distribution of tight gases: A 3D finite element simulation study. *Mar. Petroleum Geol.* 99, 75–91. doi:10.1016/j.marpetgeo.2018.10.007

Yong, R., Wu, J. F., Huang, H. Y., Xu, E. S., and Xu, B. (2022). Complex *in situ* stress states in a deep shale gas reservoir in the southern sichuan basin, China: from field stress measurements to *in situ* stress modeling. *Mar. Petroleum Geol.* 141, 105702. doi:10.1016/j.marpetgeo.2022.105702

Zhao, R., Zhao, T., Kong, Q. F., Deng, S., and Li, H. L. (2020). Relationship between fractures, stress, strike-slip fault and reservoir productivity, China Shunbei oilfield, Tarim Basin. *Carbonates Evaporites* 35, 84. doi:10.1007/s13146-020-00612-6

Zhu, Y. F., Zhang, Y. T., Zhao, X. X., Xie, Z., Wu, G. H., Li, T., et al. (2022). The fault effects on the oil migration in the ultra-deep Fuman Oilfield of the Tarim Basin, NW China. *Energies* 15, 5789. doi:10.3390/en15165789

Zoback, M. D., Barton, C. A., Brudy, M., Castillo, D. A., Finkbeiner, T., Grollimund, B. R., et al. (2003). Determination of stress orientation and magnitude in deep wells. *Int. J. Rock Mech. Min. Sci.* 40 (7-8), 1049–1076. doi:10.1016/j.ijrmms.2003.07.001

Zoback, M. D. (2007). *Reservoir geomechanics*. Cambridge: Cambridge University Press, 461.